[CANCER RESEARCH 60, 2504–2511, May 1, 2000]

A Critical Step in Metastasis: *In Vivo* Analysis of Intravasation at the Primary Tumor[1]

Jeffrey B. Wyckoff, Joan G. Jones, John S. Condeelis, and Jeffrey E. Segall[2]

Departments of Anatomy and Structural Biology [J. B. W., J. S. C., J. E. S.], Pathology [J. G. J.], and the Analytical Imaging Facility (J. S. C.), Albert Einstein College of Medicine, Bronx, New York 10461

ABSTRACT

Detailed evaluation of all steps in tumor cell metastasis is critical for evaluating the cell mechanisms controlling metastasis. Using green fluorescent protein transfectants of metastatic (MTLn3) and nonmetastatic (MTC) cell lines derived from the rat mammary adenocarcinoma 13762 NF, we have measured tumor cell density in the blood, individual tumor cells in the lungs, and lung metastases. Correlation of blood burden with lung metastases indicates that entry into the circulation is a critical step for metastasis. To examine cell behavior during intravasation, we have used green fluorescent protein technology to view these cells in time lapse images within a single optical section using a confocal microscope. *In vivo* imaging of the primary tumors of MTLn3 and MTC cells indicates that both metastatic and nonmetastatic cells are motile and show protrusive activity. However, metastatic cells show greater orientation toward blood vessels and larger numbers of host cells within the primary tumor, whereas nonmetastatic cells fragment when interacting with vessels. These results demonstrate that a major difference in intravasation between metastatic and nonmetastatic cells is detected in the primary tumor and illustrate the value of a direct visualization of cell properties *in vivo* for dissection of the metastatic process.

INTRODUCTION

Metastasis leads to poor prognosis in many cancer types. Metastasis of adenocarcinomas involves leaving the primary tumor either via lymphatics or blood vessels, transport to and arrest in a target organ, and growth of metastases in the target organ (1). Each of these steps is a multicomponent process, with potentially different tumor cell properties and molecules playing critical roles in different steps (2). As novel molecular methods are being developed to identify new genes and proteins that could contribute to specific steps, it is important to develop more detailed methods for the analysis of metastasis at the cellular level to accurately evaluate the roles of specific gene products in individual steps of metastasis. Similarly, as new therapies are developed, the effects of specific treatments on the individual steps in the metastatic cascade need to be evaluated.

The most common assays for metastatic ability *in vivo* have been end point assays. For example, i.v. injection of tumor cells (often termed "experimental metastasis"), followed by determination of the number of metastases in a target organ such as the lung, is a simple method for evaluation of arrest and growth of tumor cells in target organs (3). Detailed studies using this assay have demonstrated that extravasation *per se* tends not to be rate limiting, but that growth of metastases is inefficient (4, 5). However, this assay is limited by the introduction of a bolus (typically 100,000 cells) of *in vitro* cultivated cells in a nonphysiological manner. A more physiological approach to analysis of tumor cell metastasis makes use of the injection of tumor cells into an appropriate (orthotopic) tissue, followed by growth of a primary tumor as the source of tumor cells for metastasis. Such "spontaneous metastasis" assays are more accurate models of human disease in that they rely on growth of a primary tumor, and the tumor cells themselves then must actively leave the primary tumor and enter the vasculature (6–8). Cell lines specifically selected for high metastatic ability through use of the experimental metastasis assay are not necessarily highly metastatic in the spontaneous metastasis assay (9). Thus, for a detailed comparison of all of the various steps of metastasis, an assay such as the spontaneous metastasis assay must be used.

However, analysis of metastasis using the spontaneous metastasis assay typically measures only the growth of the primary tumor and the number of metastases that form in a target organ. The relative efficiencies for various steps in this assay have never been directly determined. Such an analysis is crucial because of the heterogeneity of tumors and tumor cell lines. Human primary tumors show extensive variation in all properties, ranging from growth and morphology of primary tumors through tumor cell density in the blood and then formation and growth of metastases. Similarly, tumor cell lines show broad variation in formation of a primary tumor and metastatic ability. As specific cell lines are manipulated to express particular activated or inhibitory oncoproteins, the effects on metastatic abilities will need to be interpreted in terms of the particular steps in the metastatic cascade that are affected. Growth of the primary tumor is simple to quantify and has been an extremely useful assay for determining proteins that are important for tumor formation. However, entry of tumor cells into the circulation is the critical first step in the metastatic cascade, and although it has been assayed in various ways (10–12), it has not been observed directly.

Because for certain tumor types and conditions there are high levels of circulating tumor cells (13, 14), it has sometimes been assumed that entry into the circulation is not a critical step in tumor cell metastasis and that formation of metastases in target organs is rate limiting. Some studies using cell-based assays indicate that tumor cell burden in the blood can correlate with poor prognosis (15, 16). However, PCR or antibody-based assays for tumor cells in the blood may not show as strong a correlation (17–20). Animal studies using well-characterized cell lines and controlled conditions are needed to evaluate the role of intravasation.

In this study, we describe a straightforward procedure for comparing intravasation, extravasation, and growth in target organs during metastasis. For two mammary adenocarcinomas, the metastatic MTLn3 and poorly metastatic MTC cell lines, we use this procedure to demonstrate that intravasation is important. We then use *in vivo* time lapse confocal microscopy of MTLn3 and MTC primary tumors expressing GFP[3] to compare the behavior of metastatic and nonmetastatic cells relative to blood vessels. We find that although both metastatic and nonmetastatic cells are motile in the primary tumor, metastatic cells are polarized toward blood vessels and nonmetastatic

Received 8/27/99; accepted 3/14/00.

The costs of publication of this article were defrayed in part by the payment of page charges. This article must therefore be hereby marked *advertisement* in accordance with 18 U.S.C. Section 1734 solely to indicate this fact.

[1] Supported by grants from the Department of Defense Army Breast Cancer Program [DAMD17-94-J-4314 (to J. E. S.) and DAMD17-96-1-6129 (to J. S. C.)] and a New York State Department of Health Empire Award (J. S. C.). J. E. S. is supported by an Established Scientist Award from the New York City affiliate of the American Heart Association.

[2] To whom requests for reprints should be addressed, at Department of Anatomy and Structural Biology, Albert Einstein College of Medicine, 1300 Morris Park Avenue, Bronx, NY 10461. Phone: (718) 430-4237; Fax: (718) 430-8996; E-mail: segall@aecom.yu.edu.

[3] The abbreviations used are: GFP, green fluorescent protein; EGF, epidermal growth factor.

cells tend to fragment during intravasation. These results provide new insights into the differences between metastatic and nonmetastatic cells and have implications for the types of assays that should be developed for prognosis.

MATERIALS AND METHODS

Cell Lines. MTLn3-GFP cells were used as described before (21). MTC-GFP cells were created using retroviral transfection of parental MTC cells with a GFP expression construct. The GFP sequence was excised from pEGFPN1 (Clontech) using NsiI and *Eco*RI and subcloned into the *Bam*HI/*Eco*RI site of pLXSN. This construct was then transfected into Phoenix cells [supplied by Vaughn Latham and Rob Singer (AECOM, Bronx, NY)] using standard methods (22, 23) and allowed to grow overnight. The supernatant was collected, spun at 1000 *rpm* for 5 min, and 1 ml was overlaid on a confluent plate of MTC cells. Positive clones were selected by neomycin selection and GFP fluorescence. Stable cells were cultured the same as parental cells, as described previously (24). Cell growth rate and morphology of transfected cells was determined to be the same as parental cells, and fluorescence was shown to remain constant for 30 passages (data not shown). Extensive histopathology studies for the MTLn3-GFP cells (21) and the MTC-GFP cells were done to confirm that their metastatic potentials were similar to the parental cell lines.

Blood Burden, Single Cells in the Lung, and Metastases. Tumor cell blood burden was determined by placing a rat with a 6-week-old tumor under isoflurane anesthesia and removing 4 ml of blood from the right atrium via heart puncture. The blood was then spun at 5000 *rpm* for 5 min, and the serum layer and buffy coat region were plated into α-MEM growth medium. The following day, plates were rinsed twice with Dulbecco's PBS (Life Technologies, Inc.) to remove RBCs, and regular growth medium was added. After 6 days, all clones in the dish were counted. To test cell viability in the collection process, blood was drawn as above from noninjected rats. Cultured MTLn3-GFP and MTC-GFP cells were removed from growth dishes using trypsin/EDTA. Ten, 100, and 1000 tumor cells were added to 1 ml of blood and 1 ml of medium, respectively. The mixtures were then centrifuged, plated, and counted as described above for blood samples derived from rats bearing tumors. There was approximately 50% recovery of tumor cells from mixtures with blood as compared with mixtures with growth medium for both cell lines.

For visualization of single cells near the surface of the lungs, the lungs were removed after blood removal and euthanization of the rat. The lungs were then placed in matTek dishes (MatTek Corporation, Ashland, MA) with 1 ml of L15 medium (Life Technologies, Inc.) to keep them moist. Ten fields from each side of both major lobes were then visualized using a $\times$60 objective on a Nikon inverted microscope. All whole single cells visible in these fields were counted. Tumor cells were shown to be countable by confirming their GFP fluorescence in the fluorescein channel and lack of fluorescence in the rhodamine channel of the Bio-Rad MRC-600 confocal microscope. A field is the 1.1-mm diameter visible area through the microscope oculars.

For measurement of metastases, excised lungs were placed in 3.7% formaldehyde, mounted in paraffin, sectioned, and stained with H&E. Slices were viewed using a $\times$20 objective, and all visible metastases in a section containing more than five cells were counted.

Imaging of Living Tumors and Their Vasculature. Tumor imaging was performed as described previously (21). Briefly, 1×10^6 cells were injected under the second nipple anterior from the tail of a Fischer 344 rat and allowed to grow for 2.5 weeks. After 2.5 weeks, the rat was placed under isoflurane anesthesia and the tumor was exposed using a simple skin flap surgery, with as little disruption of the surrounding vasculature as possible. The animal was then placed onto a Bio-Rad MRC-600 confocal microscope, using a $\times$20 objective and imaged in time lapse, with a single image being taken every minute. On average, about three different fields of each tumor were imaged for 20–30 min each.

For visualizing vasculature, 200 μl of rhodamine-dextran (2 M dalton; Sigma Chemical Co.) at 20 mg/ml in Dulbecco's PBS was injected into the tail vein of the rat after anesthesia, but before surgery. The vasculature in the tumor was then visualized using the rhodamine channel of the Bio-Rad confocal.

Quantification of Images. Time lapse movies were reconstructed using NIH Image. Movies then were viewed and evaluated for the following criteria: (*a*) cell extension and retraction; (*b*) cell locomotion (21); (*c*) cell orientation to the vasculature; and (*d*) host cell locomotion. Fields are defined as the visible area for each optical condition and are 2.4×10^5 square microns, unless indicated otherwise. For statistical purposes, an experiment is defined as a single tumor, and data are reported as the percentage of time lapse sequences for which a recorded event happens during an experiment. The velocity of cell locomotion was determined by the distance the cell moved between image frames.

Percent orientation in Table 2 was determined as the percentage of blood vessels in an imaging field with four or more directly adjacent cells polarized toward the vessel. Percent orientation was corrected for randomly polarized fields of cells by subtracting from the above value the percentage of blood vessels with both adjacent and nonadjacent cells polarized toward the vessel.

RESULTS

Entry into the Bloodstream Is an Important Step in Metastasis. To provide a quantitative comparison between blood burden and lung metastasis during spontaneous metastasis, we made use of mammary adenocarcinoma cells stably expressing GFP. The metastatic MTLn3 and nonmetastatic MTC cell lines are both derived from the Fisher rat 13762 NF mammary adenocarcinoma (25). They were transfected with GFP expression vectors and the neomycin resistance selection marker, as described by Farina *et al.* (21) and in "Materials and Methods." The cells are uniformly fluorescent, and expression of GFP does not alter their metastatic properties (see Ref. 21 and below).

Cells were injected into the mammary fat pads of Fisher 344 rats and allowed to grow for 6 weeks. To determine blood burden before filtration by any capillary bed, but with minimal perturbation of the primary tumor, the rats were anesthetized, and 4 ml of blood was withdrawn from the right atrium of the heart. The cells in the serum and buffy coat were plated in growth medium and allowed to grow for 1 week. Tumor cell colonies were identified by cell morphology and GFP fluorescence. The blood of rats carrying MTLn3 primary tumors formed about 23 colonies/4 ml of blood, which was significantly more than the blood burden of $<$1 colony/4 ml for rats carrying MTC primary tumors ($P < 0.002$; Table 1, column 2). Control experiments using defined numbers of cells mixed with blood showed a 50% plating efficiency for both cell lines. Thus, there was a significantly larger number of viable tumor cells present in the blood of rats carrying MTLn3 tumors compared with the blood of rats carrying MTC tumors. This difference was not due to larger MTLn3 tumors (Table 1, column 1). MTC tumors tended to be larger than MTLn3 tumors.

GFP fluorescence was used to identify single cells present in the lungs of the same rats used to measure blood burden. After removal of the blood, the animals were euthanized and the lungs were dissected. The lungs were viewed using a confocal microscope, and the number of fluorescent cells present in 40 high power fields was determined for each animal. Only cells showing fluorescence in the GFP channel with no fluorescence in the rhodamine channel were counted. Rats carrying MTLn3 tumors had significantly more tumor cells present in the lungs than rats carrying MTC tumors ($P < 0.003$; Table 1, column 3). In addition, for rats carrying MTLn3 tumors, comparing blood burden and fluorescent cells in the lungs in each

Table 1 *In vivo tumor cell distributions*

For MTLn3, 15 rats received injections and for MTC, 8 rats received injections. Tumor cell distributions were measured, means and SEs of the mean were calculated, and statistical significance was evaluated using the nonparametric Wilcoxon test.

	Tumor size (cm^3)	Cells in blood (per 4 ml)	Cells in lungs (per 40 HPF)	Lung mets (per section)
MTLn3	31.0 ± 5.5	22.8 ± 13.6	35.7 ± 10.1	17.9 ± 13.6
MTC	44.5 ± 9.9	0.25 ± 0.16	0.75 ± 0.75	0
P	<0.4	<0.002	<0.003	<0.003

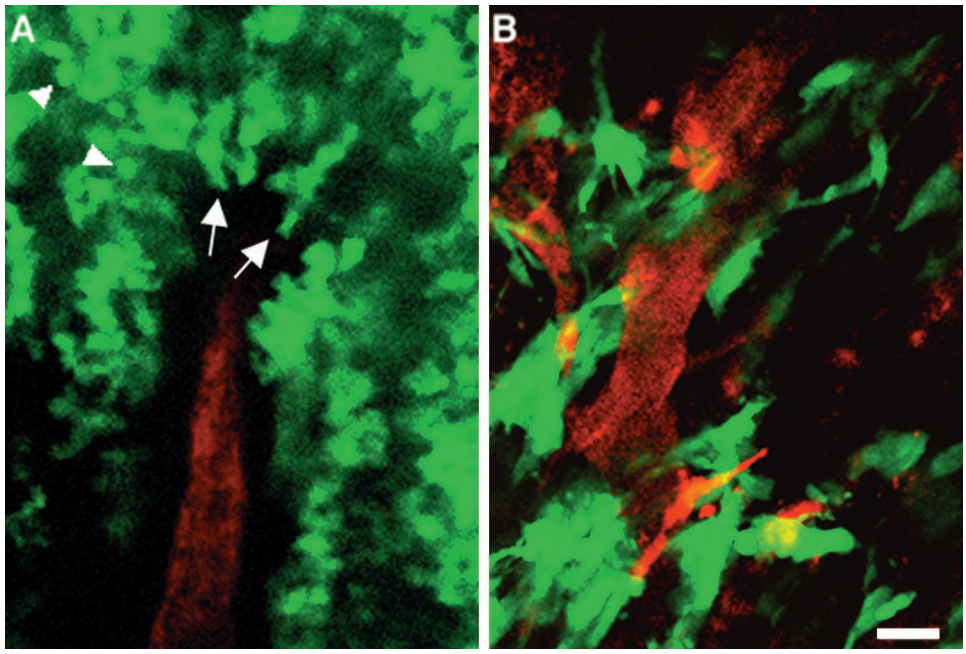

Fig. 1. MTLn3-GFP cells orient toward blood vessels, whereas MTC-GFP cells do not. Orientation of MTLn3-GFP cells (*A*) and MTC-GFP cells (*B*) to blood vessels in the primary tumor. *A*, MTLn3-GFP cells (*green*) near the vessel (*red*) are seen to orient themselves toward the vessel in an elongated fashion (*arrows*) as opposed to those away from the vessel (*arrowheads*). *B*, MTC-GFP cells (*green*) randomly associate with the vessel (*red*), and remain elongated away from the vessel. *Bar*, 25 μm.

animal there was a significant correlation (correlation coefficient, 0.86; $P < 0.0004$). However, there were no correlations with the size of the primary tumor (correlation coefficient, 0.23- 0.5; $P > 0.05$).

To evaluate metastases in the lungs of animals, sections of lungs were stained with H&E and evaluated for metastases. Rats carrying MTLn3 tumors had significantly more metastases than rats carrying MTC tumors ($P < 0.003$; Table 1, column 4). In addition, for rats carrying MTLn3 tumors there was a significant correlation between blood burden and metastases (correlation coefficient, 0.96; $P < 0.0001$).

In summary, from this analysis there was a clear correlation between tumor cell density in the blood and either numbers of single tumor cells in the lungs or metastases. This correlation was present both when comparing metastatic and nonmetastatic cell lines (MTLn3 and MTC) and when comparing MTLn3 tumors on the level of individual animals. To our knowledge, this is the first time that such a comparison has been performed on a single animal basis. The presence of a correlation between blood burden and both single cells, as well as metastases in the lungs, indicates that entry into the blood is important for metastasis of cells derived from the 13762 NF mammary adenocarcinoma. These data suggest that a more detailed analysis of cell behavior in the primary tumor is important for determining the properties that enable MTLn3 cells to gain access to the circulation. To perform such studies, we made use of the GFP expression of these cell lines to perform intravital imaging of the primary tumors.

Intravital Imaging of MTLn3 and MTC Primary Tumors

Metastatic Cells Are Oriented toward Blood Vessels. As reported previously (26), MTLn3-GFP cells form loose clusters of rounded, nonpolarized cells in the primary tumor, whereas MTC-GFP cells are elongated and polarized in tight sheets. This was confirmed by both histopathology sections and intravital imaging. However, around blood vessels, MTLn3-GFP cells were elongated and polarized toward blood vessels. In Fig. 1*A*, MTLn3-GFP cells (*green*) are elongated and polarized (*arrows*) toward the vessel (*red*), whereas cells away from the vessel are rounded (*arrowheads*). Fig. 1*B* shows MTC-GFP cells (*green*) that are elongated throughout the field of view, with cell elongation occurring independent of the vessel positions. Overall, for MTLn3 tumors, 57 +/− 6% of all vessels had polarized cells near them, compared with 24 +/− 4% for vessels in MTC-GFP tumors (Table 2, column 1). This suggests that there is a vessel-mediated effect on MTLn3 cells that results in orientation toward the vessels.

The differences in cell locomotion (translocation) and protrusiveness between metastatic and nonmetastatic cells are much smaller in the primary tumor. During a time lapse sequence, cells within the primary tumor can be detected extending and retracting processes, as well as translocating. Both protrusiveness and translocation were reported previously for MTLn3-GFP cells in the primary tumor (21), and similar phenomena were observed in the MTC-GFP primary tumors. For the MTLn3-GFP tumors, cell protrusion and retraction occur in 62% of tumors compared with 47% for MTC tumors (Table 2, column 2). Fig. 2 shows the protrusive activity of an MTC-GFP tumor cell. The cell extends a small protrusion (Fig. 2*B*), which then enlarges (Fig. 2*C*). The movement of the leading edge of this cell was 3.8 μm/min during maximum rate of extension, consistent with the average rate of movement seen for MTLn3 and MTC cells (see below). For MTLn3-GFP cells, the most obvious shape changes occur at the periphery of vessels where the cells are elongated, whereas for MTC cells protrusion and locomotion occur randomly relative to vessels.

Cell translocation occurs much less frequently in both tumor types. As opposed to protrusive activity, only a small fraction of the cells within a primary tumor translocate at a given time. MTLn3-GFP cell

Table 2 *In vivo analysis of tumor cell behavior*

The percentage of tumor time lapse sequences with cells showing the specified behavior is given, together with SE of the mean. Orientation was determined as the percentage of blood vessels in an imaging field with four or more adjacent cells polarized toward the vessel (see "Materials and Methods"). For MTLn3 tumors, a total of 122 fields from 45 tumors containing 163 vessels was analyzed. For MTC tumors, a total of 63 fields from 24 tumors with 97 vessels was analyzed.

	Orientation	Protrusion	Translocation	Fragmentation
MTLn3	57% ± 6%	62% ± 5%	17% ± 4%	6% ± 2%
MTC	24% ± 4%	47% ± 7%	10% ± 4%	32% ± 5%
P	<0.0001	<0.04	<0.07	<0.001

locomotion within the primary tumor, as reported previously and observed with more tumors here, is seen as a linear movement. The cell shown in Fig. 3 moves on a linear path at a speed of 3.6 μm/min. This type of movement is seen in 17% of all MTLn3 tumors and 10% of MTC tumors (Table 2, column 3). The MTC-GFP cell shown in Fig. 4 moves at a rate of 3.6 μm/min. The average velocities of movement of MTLn3 (3.4 μm/min, 12 cells) and MTC (3.7 μm/min, 7 cells) were similar.

Nonmetastatic Cells Demonstrate Extensive Fragmentation. MTC-GFP tumor cells show a significantly greater number of cell fragmentation events compared with MTLn3-GFP tumor cells. Fragments of cells are visualized breaking from cell protrusions and moving away at an accelerated rate of speed (Fig. 5). In Fig. 5, a fragment is seen attached to a cell extension (*A*), then breaks off and moves away from the cell (*B* and *C*). The initial rate of protrusion of the extension was 2.8 μm/min, but the fragment speed of movement is 11–15 μm/min. This was observed in 32% of MTC-GFP tumors compared with 6% of MTLn3-GFP tumors (Table 2, column 4). In a number of cases, the fragmentation was seen to occur in blood vessels. The higher velocity of the fragment is consistent with passive flow in the blood because the velocity is too high for cell locomotion (maximum about 4 μm/min) and close to the velocity of blood flow in small vessels.

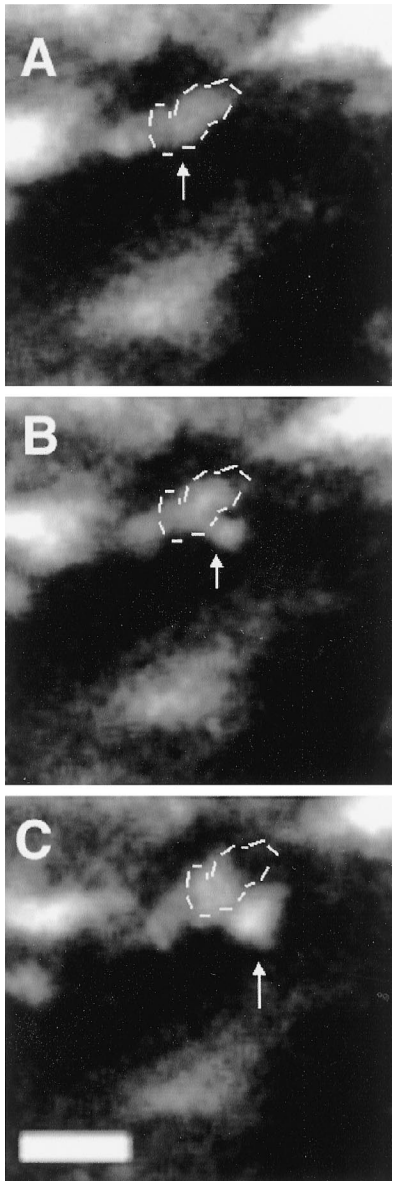

Fig. 2. MTC-GFP cells are able to move in a primary tumor by first sending out a thin leading edge protrusion through a small space. Protrusive movement of a whole MTC-GFP cell within the primary tumor viewed in a single optical section *in situ*. *A*, initial position of cell. *B*, initial extension of protrusion. *C*, further protrusion. The *outline* shows starting position. The images are 5 min apart. *Bar*, 25 μm.

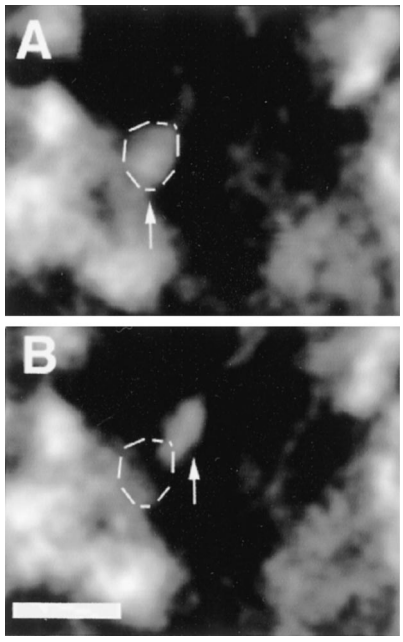

Fig. 3. MTLn3-GFP cells exhibit linear translocation *in situ*. Movement of a MTLn3-GFP cell in a single optical section of the primary tumor. The cell moved over a distance of 22 μm. *A*, the cell seen in its starting position (*outlined*, with *arrow*). *B*, cell has moved to a new position 6 min later (*arrow*). Its starting position is *outlined*. The cell moved at an average velocity of 3.6 μm/min. *Bar*, 25 μm.

More Motile Host Cells Are Visualized in Metastatic Tumors. During fluorescent imaging of GFP-tagged tumor cells, we have observed nonfluorescent cells moving against the fluorescent tumor cell background as they block and scatter fluorescence from the tumor cells (Fig. 6). It is likely that these are host immune system cells for the following reasons: (*a*) the cells are not fluorescent; (*b*) the cells are smaller than the tumor cells; and (*c*) the speed of movement is relatively high (on the order of 10 μm/min). Although host cells were observed at similar frequencies in MTLn3 and MTC tumors (28% and 23%, respectively; Table 3, column 1), there was a significant difference in the number of host cells observed. For MTLn3-GFP tumors, there was an average of 11 host cells observed per field, compared with 2 host cells/field for MTC-GFP tumors (Table 3, column 2). The increased numbers of host cells may aid in either polarizing the tumor cells toward blood vessels or in generating pores through which tumor cells can intravasate.

Movies of the data from which the figures were derived are available.[4]

DISCUSSION

We present here the combination of two novel analyses of tumor cell metastasis: (*a*) a steady-state analysis of tumor cell distributions in individual animals; and (*b*) *in vivo* imaging of cell behavior in primary tumors. The steady-state analysis of tumor cell distributions indicates that entry into the vasculature is an important step that contributes to differences in metastasis between MTLn3- and MTC-

[4] http://www.aecom.yu.edu/asb/segall/segall.htm.

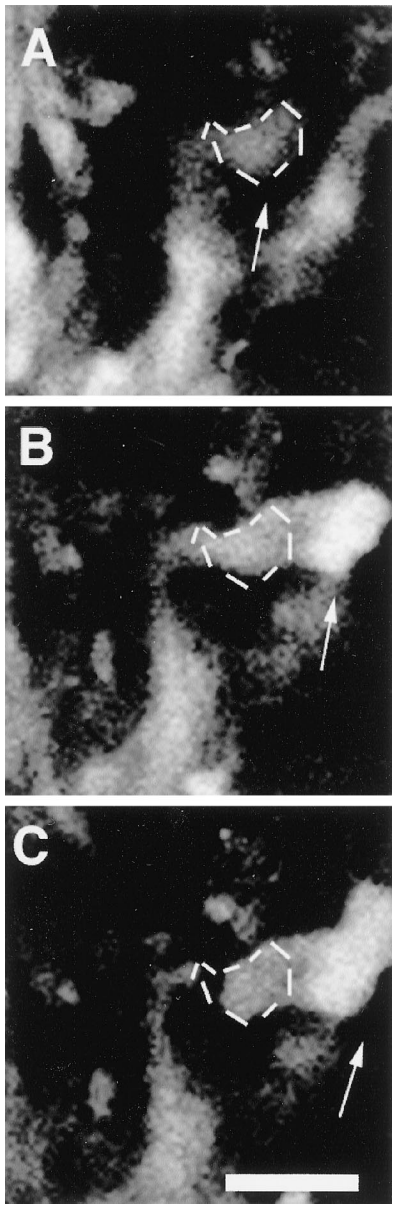

Fig. 4. MTC-GFP cells exhibit linear translocation *in situ*. Movement of a MTC-GFP cell in a single optical section of the primary tumor. *A*, cell is shown *outlined* in its starting position (*arrow*). *B* and *C*, images showing a progressively linear movement (*arrows*). The *outline* shows the original position. The cell moved at an average speed of 3.6 μm/min. The images are 4 min apart. *Bar*, 25 um.

derived tumors. To define the mechanisms behind this difference, we used confocal microscopy of GFP-transfected cells in anesthetized animals. MTLn3 tumor cells were more highly oriented around blood vessels compared with MTC tumor cells. Protrusive activity and random cell movement were similar. However, MTC tumor cells were much more likely to form fragments. In addition, more host cells were detected in MTLn3 tumors compared with MTC tumors.

Steady-State Analysis of Metastasis. We have used a steady-state analysis of tumor cell distributions in individual animals to develop a general method for comparing intravasation with growth in the lungs during metastasis. We have found that although the primary tumor sizes formed are similar, rats carrying the more metastatic MTLn3 tumors have about 90 times more cells in the blood than rats carrying MTC tumors. Although previous studies had demonstrated that MTC cells injected i.v. form few metastases in the lungs (27), this is the first demonstration that MTC cells are also unable to effectively enter the circulation.

There are two limitations in our estimate of tumor cell density in the blood. First, because we are using colony counts, each clump of tumor cells would be counted as a single colony-forming unit, or cell (10, 12, 14). Second, the cells must be able to grow *in vitro*. Given that these tumor cell lines grow well *in vitro* before injection into the animal to form a tumor, the latter limitation is not significant. Reconstruction experiments *in vitro* indicate that exposure to blood *per se* produces a roughly 50% reduction in plating efficiency for both cell lines. Thus, our estimate of tumor cell density in the blood may be an underestimate of the true number.

To determine whether metastasis of the MTLn3 cells could be dependent on intravasation as well, we compared the tumor cell density in the blood with single cells and metastases in the lungs for each rat carrying MTLn3 tumors. We found a significant correlation between blood density and single cells or metastases in the lungs. This result suggests that entry into or survival in the vasculature is an inefficient step for MTLn3 cells as well as for MTC cells. In addition, for animals carrying MTLn3 tumors, the number of lung metastases is

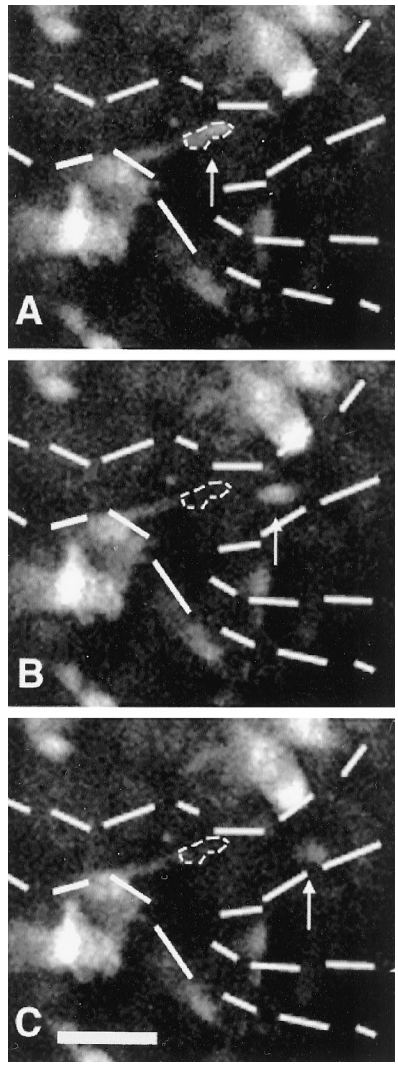

Fig. 5. The protrusions of MTC-GFP cells *in situ* are seen to break off from the cell body and move away rapidly. *A*, cell protrusion before being broken off (*arrow*). *B* and *C*, fragment broken off from the protrusion (*arrows*). The *outline* shows starting position. Speed of fragment after breaking away from protrusion suggests movement into vascular flow (*large hash marks* delineate vessel). The initial speed of protrusion is 2.8 μm/min; after release it increases to 11–15 μm/min. The images are 1 min apart. *Bar*, 25 μm.

less than would be expected given the single cell density in the lungs. This indicates that growth of metastases in the lungs is also inefficient, as has been well recognized (28–32).

***In Vivo* Imaging of the Primary Tumor.** Given the results above indicating that intravasation is an important difference between metastatic and nonmetastatic tumors, a more detailed analysis of the cell behavior in the primary tumor becomes important. A number of researchers have made use of GFP (5, 21, 33–35) or lacZ (36–40) expression to increase the sensitivity of observations of disseminated tumor cells in target organs. We made use of techniques developed to follow individual tumor cells in primary tumors with an intact blood supply. By using a confocal scanning microscope to image cells that stably express green fluorescent protein, we are able to follow cell movements over 30 min. These studies provide the first comparison of *in vivo* cell behavior at the primary tumor with metastatic ability.

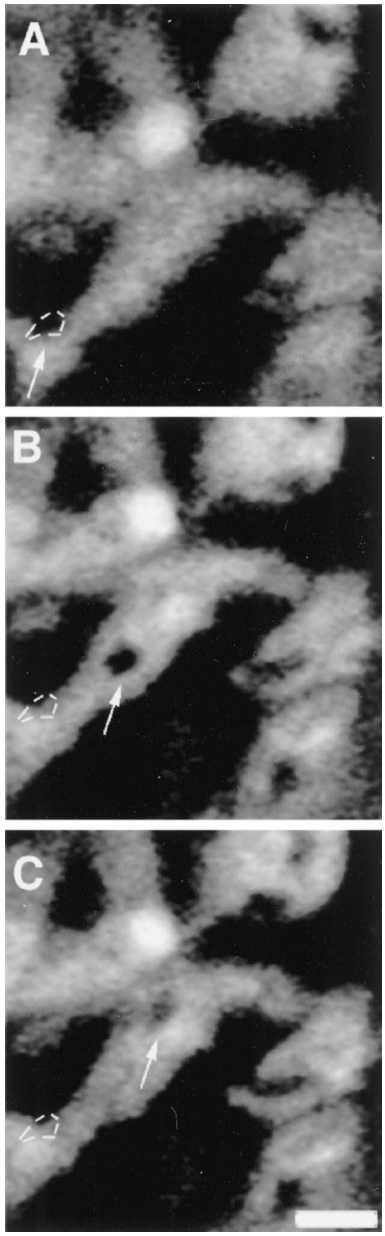

Fig. 6. Host cells can be visualized as *shadows* on top of *white* fluorescent cells in the primary tumor. Host cell movement over MTLn3-GFP cells in a single optical section of the primary tumor viewed *in situ*. *A-C*, host cells are seen as *black shapes* (*arrows*) moving over fluorescent tumor cells (MTLn3-GFP). The *outline* shows the starting position. Host cells move at 7.7 μm/min, and the images are 7 min apart. *Bar*, 25 μm.

Table 3 *Host cells in tumor*

The percentage of tumor time lapse sequences with cells showing the specified behavior is given, together with SE of the mean. For MTLn3 tumors, a total of 122 fields from 45 tumors was analyzed. For MTC tumors, a total of 63 fields from 24 tumors was analyzed.

	Tumors with host cells visualized	Number of host cells per field
MTLn3	28% ± 5%	11.18 ± 1.33
MTC	23% ± 6%	1.8 ± 0.19
P	<0.45	$<1 \times 10^{-8}$

There are three major differences between the MTLn3 and MTC primary tumors: increased cell orientation toward blood vessels in MTLn3 tumors, increased fragmentation of cells in MTC tumors, and increased numbers of putative host cells in MTLn3 tumors. There are not as dramatic differences in protrusive activity and random cell translocation between these tumors.

Increased cell orientation of MTLn3 cells toward blood vessels could increase the efficiency with which they can then intravasate. The increased orientation could result in directed movement into the blood vessel and more cells moving into the blood. The orientation could be induced by chemoattractant diffusing from the blood vessel. Growth factors, including EGF or platelet-derived growth factor, are present in platelets and smooth muscle cells (*e.g.*, see Refs. 41–44). Release of growth factors from these cells or endothelial cells could provide a gradient that would produce a chemotactic response. MTLn3 cells are chemotactic toward EGF *in vitro*, whereas MTC cells are not (45). MTLn3 cells express more EGF receptors than MTC cells (46), and expression of the EGF receptor in MTC cells increases chemotactic responses to EGF and metastatic ability (47, 48). Expression of the EGF receptor and other EGF receptor homologues, such as ErbB2, have been correlated with poor prognosis. It is possible that chemotactic signaling mediated by the EGF receptor is important in enhancing metastatic capability in addition to the well characterized effects of EGF receptor signaling on mitogenesis.

The increased fragmentation of MTC cells compared with MTLn3 cells provides an additional mechanism by which viable cell number in the blood might be low for MTC cells. In some cases, we have identified fragmentation occurring during intravasation. If the shear forces in the blood vessels are causing MTC cells to fragment as they enter the blood vessel, that event will eliminate the possibility of metastasis. The increased susceptibility to fragmentation of MTC cells could reflect a lack of orientation toward the blood vessel and slow traversal of the endothelium due to a reduced chemotactic response, as suggested above. Morris *et al.* (49) have reported fragmentation of tumor cells injected i.v. and then viewed during extravasation into microvascular beds. At the extravasation stage of metastasis, fragmentation of both metastatic and nonmetastatic cells may occur if cells do not rapidly polarize and exit the blood vessel.

The observation of fragmentation of poorly metastatic cells has important implications for biochemical or molecular-based assays of blood. Given that cell fragments would contain tumor protein and DNA, immunological assays for tumor proteins or PCR-based assays for tumor DNA would be positive, although the fragments would be unable to metastasize. In that event, PCR- or protein-based assays of blood samples might not be useful for predicting metastases. A cell-based assay that evaluates the size of cells may be a more powerful predictor of poor prognosis.

An unexpected dividend of the GFP-based imaging was the ability to image motile nonfluorescent cells against the background of fluorescent cells. We have observed small, rapidly moving cells that are likely to be host immune cells. H&E sections of the primary tumor confirm that host immune cells are present in the primary tumor (data

not shown), supporting this interpretation. Increased numbers of immune system cells could contribute to increased metastasis by production of chemotactic factors or degradation of extracellular matrix barriers (*e.g.,* see Refs. 50–54).

Breast cancer both in humans and in animal models including the MTLn3 cells (21, 55) spreads to lymph nodes, indicating that the lymphatic circulation can also be important for tumor cell metastasis. In our *in vivo* studies, in cases in which tumor cells are oriented or exiting the tumor in the absence of a labeled blood vessel, it is possible that the cells are interacting with lymphatics. Comparing the *in vivo* behavior of tumor cells around lymphatics with their behavior around blood vessels awaits development of an appropriate *in vivo* marker for lymphatics.

In summary, we have demonstrated a method for providing a more detailed analysis of metastatic ability of tumor cells. The method is straightforward and should be valuable in determining the contributions to metastasis of specific proteins expressed in tumor cells. In addition, our *in vivo* analysis of tumor cell behavior has indicated that cell orientation toward blood vessels may be a characteristic of metastatic cells and that poorly metastatic cells can fragment during intravasation. These distinctions may prove important in choosing appropriate assays for predicting disease progression.

ACKNOWLEDGMENTS

We gratefully acknowledge the staff of the Analytical Imaging Facility at Albert Einstein College of Medicine for assistance in intravital imaging and image analysis, Dr. Maryse Bailly for aid in the generation of rat tumors, and the laboratories of Drs. John S. Condeelis and Jeffrey E. Segall for scientific and critical input.

REFERENCES

1. Fidler, I. J. Critical determinants of cancer metastasis: rationale for therapy. Cancer Chemother. Pharmacol., *43* (Suppl.)*:* S3–S10, 1999.
2. Price, J. T., Bonovich, M. T., and Kohn, E. C. The biochemistry of cancer dissemination. Crit. Rev. Biochem. Mol. Biol., *32:* 175–253, 1997.
3. Price, J. E. The biology of cancer metastasis. Prog. Clin. Biol. Res., *354A:* 237–255, 1990.
4. Morris, V. L., Schmidt, E. E., MacDonald, I. C., Groom, A. C., and Chambers, A. F. Sequential steps in hematogenous metastasis of cancer cells studied by *in vivo* videomicroscopy. Invasion Metastasis, *17:* 281–296, 1997.
5. Naumov, G. N., Wilson, S. M., MacDonald, I. C., Schmidt, E. E., Morris, V. L., Groom, A. C., Hoffman, R. M., and Chambers, A. F. Cellular expression of green fluorescent protein, coupled with high- resolution *in vivo* videomicroscopy, to monitor steps in tumor metastasis. J. Cell Sci., *112:* 1835–1842, 1999.
6. Kerbel, R. S. What is the optimal rodent model for anti-tumor drug testing? Cancer Metastasis Rev., *17:* 301–304, 1998.
7. Killion, J. J., Radinsky, R., and Fidler, I. J. Orthotopic models are necessary to predict therapy of transplantable tumors in mice. Cancer Metastasis Rev., *17:* 279–284, 1998.
8. Price, J. E. Analyzing the metastatic phenotype. J. Cell. Biochem., *56:* 16–22, 1994.
9. Weiss, L., Mayhew, E., Rapp, D. G., and Holmes, J. C. Metastatic inefficiency in mice bearing B16 melanomas. Br. J. Cancer, *45:* 44–53, 1982.
10. Glaves, D. Detection of circulating metastatic cells. Prog. Clin. Biol. Res., *212:* 151–167, 1986.
11. Butler, T. P., and Gullino, P. M. Quantitation of cell shedding into efferent blood of mammary adenocarcinoma. Cancer Res., *35:* 512–516, 1975.
12. Liotta, L. A., Kleinerman, J., and Saidel, G. M. Quantitative relationships of intravascular tumor cells, tumor vessels, and pulmonary metastases following tumor implantation. Cancer Res., *34:* 997–1004, 1974.
13. Tarin, D., Price, J. E., Kettlewell, M. G., Souter, R. G., Vass, A. C., and Crossley, B. Mechanisms of human tumor metastasis studied in patients with peritoneovenous shunts. Cancer Res., *44:* 3584–3592, 1984.
14. Glaves, D., Huben, R. P., and Weiss, L. Haematogenous dissemination of cells from human renal adenocarcinomas. Br. J. Cancer, *57:* 32–35, 1988.
15. Racila, E., Euhus, D., Weiss, A. J., Rao, C., McConnell, J., Terstappen, L. W. M. M., and Uhr, J. W. Detection and characterization of carcinoma cells in the blood. Proc. Natl. Acad. Sci. USA, *95:* 4589–4594, 1998.
16. Denis, M. G., Lipart, C., Leborgne, J., LeHur, P. A., Galmiche, J. P., Denis, M., Ruud, E., Truchaud, A., and Lustenberger, P. Detection of disseminated tumor cells in peripheral blood of colorectal cancer patients. Int. J. Cancer, *74:* 540–544, 1997.
17. Kawamata, H., Uchida, D., Nakashiro, K., Hino, S., Omotehara, F., Yoshida, H., and Sato, M. Haematogenous cytokeratin 20 mRNA as a predictive marker for recurrence in oral cancer patients. Br. J. Cancer, *80:* 448–452, 1999.
18. Gao, C. L., Maheshwari, S., Dean, R. C., Tatum, L., Mooneyhan, R., Connelly, R. R., McLeod, D. G., Srivastava, S., and Moul, J. W. Blinded evaluation of reverse transcriptase-polymerase chain reaction prostate-specific antigen peripheral blood assay for molecular staging of prostate cancer. Urology, *53:* 714–721, 1999.
19. de la Taille, A., Olsson, C. A., and Katz, A. E. Molecular staging of prostate cancer: dream or reality? Oncology (Basel), *13:* 187–194, 1999.
20. Peck, K., Sher, Y. P., Shih, J. Y., Roffler, S. R., Wu, C. W., and Yang, P. C. Detection and quantitation of circulating cancer cells in the peripheral blood of lung cancer patients. Cancer Res., *58:* 2761–2765, 1998.
21. Farina, K. L., Wyckoff, J., Rivera, J., Lee, H., Segall, J. E., Condeelis, J. S., and Jones, J. G. Cell motility of tumor cells visualized in living intact primary tumors using green fluorescent protein. Cancer Res., *58:* 2528–2532, 1998.
22. Miller, A. D., and Rosman, G. J. Improved retroviral vectors for gene transfer and expression. Biotechniques, *7:* 980–982, 1989.
23. Kinsella, T. M., and Nolan, G. P. Episomal vectors rapidly and stably produce high-titer recombinant retrovirus. Hum. Gene Ther., *7:* 1405–1413, 1996.
24. Segall, J. E., Tyerech, S., Boselli, L., Masseling, S., Helft, J., Chan, A., Jones, J., and Condeelis, J. EGF stimulates lamellipod extension in metastatic mammary adenocarcinoma cells by an actin-dependent mechanism. Clin. Exp. Metastasis, *14:* 61–72, 1996.
25. Neri, A., Welch, D., Kawaguchi, T., and Nicolson, G. L. Development and biologic properties of malignant cell sublines and clones of a spontaneously metastasizing rat mammary adenocarcinoma. J. Natl. Cancer Inst., *68:* 507–517, 1982.
26. Shestakova, E. A., Wyckoff, J., Jones, J., Singer, R. H., and Condeelis, J. Correlation of β-actin messenger RNA localization with metastatic potential in rat adenocarcinoma cell lines. Cancer Res., *59:* 1202–1205, 1999.
27. Welch, D. R., Neri, A., and Nicolson, G. L. Comparison of "spontaneous" and "experimental" metastasis using rat 13762 mammary adenocarcinoma metastatic cell clones. Invasion Metastasis, *3:* 65–80, 1983.
28. Glaves, D. Correlation between circulating cancer cells and incidence of metastases. Br. J. Cancer, *48:* 665–673, 1983.
29. Weiss, L., and Ward, P. M. Lymphogenous and hematogenous metastasis of Lewis lung carcinoma in the mouse. Int. J. Cancer, *40:* 570–574, 1987.
30. Liotta, L. A., and DeLisi, C. Method for quantitating tumor cell removal and tumor cell-invasive capacity in experimental metastases. Cancer Res., *37:* 4003–4008, 1977.
31. Koop, S., Schmidt, E. E., MacDonald, I. C., Morris, V. L., Khokha, R., Grattan, M., Leone, J., Chambers, A. F., and Groom, A. C. Independence of metastatic ability and extravasation: metastatic ras-transformed and control fibroblasts extravasate equally well. Proc. Natl. Acad. Sci. USA, *93:* 11080–11084, 1996.
32. Lin, W. C., Pretlow, T. P., Pretlow, T. G., and Culp, L. A. Development of micrometastases: earliest events detected with bacterial lacZ gene-tagged tumor cells. J. Natl. Cancer Inst., *19:* 82: 1497–1503, 1990.
33. Chishima, T., Miyagi, Y., Wang, X., Baranov, E., Tan, Y., Shimada, H., Moossa, A. R., and Hoffman, R. M. Metastatic patterns of lung cancer visualized live and in process by green fluorescence protein expression. Clin. Exp. Metastasis, *15:* 547–552, 1997.
34. Kan, Z., and Liu, T. J. Video microscopy of tumor metastasis: using the green fluorescent protein (GFP) gene as a cancer-cell-labeling system. Clin. Exp. Metastasis, *17:* 49–55, 1999.
35. Hoffman, R. M. Orthotopic transplant mouse models with green fluorescent protein-expressing cancer cells to visualize metastasis and angiogenesis. Cancer Metastasis Rev., *17:* 271–277, 1998.
36. Kobayashi, K., Nakanishi, H., Inada, K., Fujimitsu, Y., Yamachika, T., Shirai, T., and Tatematsu, M. Growth characteristics in the initial stage of micrometastasis formation by bacterial LacZ gene-tagged rat prostatic adenocarcinoma cells. Jpn. J. Cancer Res., *87:* 1227–1234, 1996.
37. McLeskey, S. W., Zhang, L., Kharbanda, S., Kurebayashi, J., Lippman, M. E., Dickson, R. B., and Kern, F. G. Fibroblast growth factor overexpressing breast carcinoma cells as models of angiogenesis and metastasis. Breast Cancer Res. Treat., *39:* 103–117, 1996.
38. Kruger, A., Schirrmacher, V., and Khokha, R. The bacterial lacZ gene: an important tool for metastasis research and evaluation of new cancer therapies. Cancer Metastasis Rev., *17:* 285–294, 1998.
39. Culp, L. A., Lin, W. C., Kleinman, N. R., Campero, N. M., Miller, C. J., and Holleran, J. L. Tumor progression, micrometastasis, and genetic instability tracked with histochemical marker genes. Prog. Histochem. Cytochem., *33:* 11–15, 1998.
40. Kobayashi, K., Nakanishi, H., Masuda, A., Tezuka, N., Mutai, M., and Tatematsu, M. Sequential observation of micrometastasis formation by bacterial lacZ gene-tagged Lewis lung carcinoma cells. Cancer Lett., *112:* 191–198, 1997.
41. Calabro, A., Orsini, B., Renzi, D., Papi, L., Surrenti, E., Amorosi, A., Herbst, H., Milani, S., and Surrenti, C. Expression of epidermal growth factor, transforming growth factor-α and their receptor in the human oesophagus. Histochem. J., *29:* 745–758, 1997.
42. Peoples, G. E., Blotnick, S., Takahashi, K., Freeman, M. R., Klagsbrun, M., and Eberlein, T. J. T lymphocytes that infiltrate tumors and atherosclerotic plaques produce heparin-binding epidermal growth factor-like growth factor and basic fibroblast growth factor: a potential pathologic role. Proc. Natl. Acad. Sci. USA, *92:* 6547–6551, 1995.
43. Kume, N., and Gimbrone, M. J. Lysophosphatidylcholine transcriptionally induces growth factor gene expression in cultured human endothelial cells. J. Clin. Invest., *93:* 907–911, 1994.
44. Dluz, S. M., Higashiyama, S., Damm, D., Abraham, J. A., and Klagsbrun, M. Heparin-binding epidermal growth factor-like growth factor expression in cultured fetal human vascular smooth muscle cells. Induction of mRNA levels and secretion of active mitogen. J. Biol. Chem., *268:* 18330–18334, 1993.

45. Wyckoff, J. B., Insel, L., Khazaie, K., Lichtner, R. B., Condeelis, J. S., and Segall, J. E. Suppression of ruffling by EGF in chemotactic cells. Exp. Cell Res., *242:* 100–109, 1998.
46. Kaufmann, A. M., Khazaie, K., Wiedemuth, M., Rohde-Schulz, B., Ullrich, A., Schirrmacher, V., and Lichtner, R. B. Expression of epidermal growth factor receptor correlates with metastatic potential of 13762NF rat mammary adenocarcinoma cells. Int. J. Oncol., *4:* 1149–1155, 1994.
47. Lichtner, R. B., Kaufmann, A. M., Kittmann, A., Rohde-Schulz, B., Walter, J., Williams, L., Ullrich, A., Schirrmacher, V., and Khazaie, K. Ligand mediated activation of ectopic EGF receptor promotes matrix protein adhesion and lung colonization of rat mammary adenocarcinoma cells. Oncogene, *10:* 1823–1832, 1995.
48. Kaufmann, A. M., Lichtner, R. B., Schirrmacher, V., and Khazaie, K. Induction of apoptosis by EGF receptor in rat mammary adenocarcinoma cells coincides with enhanced spontaneous tumour metastasis. Oncogene, *13:* 2349–2358, 1996.
49. Morris, V. L., MacDonald, I. C., Koop, S., Schmidt, E. E., Chambers, A. F., and Groom, A. C. Early interactions of cancer cells with the microvasculature in mouse liver and muscle during hematogenous metastasis: videomicroscopic analysis. Clin. Exp. Metastasis, *11:* 377–390, 1993.
50. Ohtani, H. Stromal reaction in cancer tissue: pathophysiologic significance of the expression of matrix-degrading enzymes in relation to matrix turnover and immune/inflammatory reactions. Pathol. Int., *48:* 1–9, 1998.
51. Dong, Z., Kumar, R., Yang, X., and Fidler, I. J. Macrophage-derived metalloelastase is responsible for the generation of angiostatin in Lewis lung carcinoma. Cell, *88:* 801–810, 1997.
52. Zeng, Z. S., and Guillem, J. G. Colocalisation of matrix metalloproteinase-9-mRNA and protein in human colorectal cancer stromal cells. Br. J. Cancer, *74:* 1161–1167, 1996.
53. Christensen, L., Wiborg, S. C., Heegaard, C. W., Moestrup, S. K., Andersen, J. A., and Andreasen, P. A. Immunohistochemical localization of urokinase-type plasminogen activator, type-1 plasminogen-activator inhibitor, urokinase receptor and α(2)-macroglobulin receptor in human breast carcinomas. Int. J. Cancer, *66:* 441–452, 1996.
54. Nielsen, B. S., Timshel, S., Kjeldsen, L., Sehested, M., Pyke, C., Borregaard, N., and Dano, K. 92 kDa type IV collagenase (MMP-9) is expressed in neutrophils and macrophages but not in malignant epithelial cells in human colon cancer. Int. J. Cancer, *65:* 57–62, 1996.
55. Edmonds, B. T., Wyckoff, J., Yeung, Y. G., Wang, Y., Stanley, E. R., Jones, J., Segall, J., and Condeelis, J. Elongation factor-1α is an overexpressed actin binding protein in metastatic rat mammary adenocarcinoma. J. Cell Sci., *109:* 2705–2714, 1996.